Density-matrix formalism for the photoion-electron entanglement in atomic photoionization

T. Radtke* and S. Fritzsche†
Institut für Physik, Universität Kassel, D-34132 Kassel, Germany

A. Surzhykov
Max-Planck-Institut für Kernphysik, Saupfercheckweg 1, D-69117 Heidelberg, Germany

(Received 21 June 2006; published 27 September 2006)

The density-matrix theory, based on Dirac's relativistic equation, is applied for studying the entanglement between the photoelectron and residual ion in the course of the photoionization of atoms and ions. In particular, emphasis is placed on deriving the final-state density matrix of the overall system "photoion+electron," including interelectronic effects and the higher multipoles of the radiation field. This final-state density matrix enables one immediately to analyze the change of entanglement as a function of the energy, angle and the polarization of the incoming light. Detailed computations have been carried out for the $5s$ photoionization of neutral strontium, leading to a photoion in a $5s\,^2S\ J_f=1/2$ level. It is found that the photoion-electron entanglement decreases significantly near the ionization threshold and that, in general, it depends on both the photon energy and angle. The possibility to extract photoion-electron pairs with a well-defined degree of entanglement may have far-reaching consequences for quantum information and elsewhere.

DOI: 10.1103/PhysRevA.74.032709 PACS number(s): 32.80.Fb, 31.25.−v, 03.67.Mn

I. INTRODUCTION

Since the early days of quantum mechanics, the—often counterintuitive—implications of this theory have been the subject of many controversial discussions. For instance, in the famous gedanken experiment by Einstein, Podolsky, and Rosen [1] it was shown that quantum mechanics allows for nonlocal correlations between the outcomes of two (or more) measurements of spatially separated quantum systems. Indeed, these strange quantum mechanical correlations violate the principle of locality and led Einstein to his belief that quantum mechanics is an incomplete theory. In contrast, Schrödinger identified these correlations as one of the key features of quantum mechanics and introduced the name *quantum entanglement* for this phenomenon [2].

Today, the entanglement in composite quantum systems plays an important role in quite different areas of physics, from the basic research up to the first successful devices in the new field of quantum engineering. In quantum information [3], in particular, several applications of quantum entanglement have been developed such as superdense coding [4], quantum cryptography [5], and efficient quantum algorithms [6,7]. However, despite the remarkable progress in the last decade, the experimental implementation of quantum information protocols is still a challenge owing to the fragile nature of quantum entanglement. In many experimental and theoretical studies, therefore, much attention has been paid recently to those (quantum) processes which can be utilized in order to observe and manipulate the entanglement in quantum systems.

One such process which allows for the creation and manipulation of entanglement is the photoionization of atoms and ions as suggested recently by Kim and co-workers [8]. For the case of two hydrogenlike and heliumlike ions, these authors considered the question how the spin entanglement between the photoelectron and the remaining photoion is affected in the course of the ionization process. Applying the independent particle model (IPM) and the dipole approximation for the electron-photon interaction it was shown, for example, that the entanglement of an initial triplet state $|nsms\,^3S\rangle$ of two bound electrons can be modified significantly during the photoionization with circularly polarized light. These studies by Kim *et al.* have been extended by us in Ref. [9], where we applied the density-matrix theory in order to analyze the influence of the geometry as well as the relativistic and nondipole effects in the electron-photon interaction. No attempt, however, was made so far to explore the role of the electron-electron interaction in the change and control of entanglement in atomic photoionization processes. This interaction, which is inherent to all many-electron atoms and ions may play an important role in nowadays experiments with trapped many-electron ions and may significantly change the spin properties of the emitted photoelectrons and the residual ions.

In this contribution, we apply the density matrix theory for studying the change in the entanglement between the photoelectron and residual ion in the course of the photoionization. To this end, we generalized the formalism from Ref. [9] for many-electron atoms, including the effects of the electron-electron interaction and the higher multipoles of the radiation field. For the sake of simplicity, however, we restricted our considerations to the *direct* photoionization of an ns valence electron, leaving the photoion in a well-defined $^2S_{1/2}$ spin state which can be interpreted as a single qubit. This restriction excludes all known resonance phenomena in the photoionization of atoms and ions as well as the question of how to deal with the residual ion in those cases, where the final states have a total angular momentum $J\neq 1/2$.

The paper is organized as follows. In Sec. II, we explain the main steps in deriving the final-state density matrix for the system photoelectron+ion, starting from a well-defined

*Electronic address: t.radtke@physik.uni-kassel.de
†Electronic address: s.fritzsche@physik.uni-kassel.de

geometry and initial setup of the photoionization process. This final-state density matrix describes the spin states of both, the emitted photoelectron and the residual ion. It is shown, in particular, how this matrix can be traced back to the (reduced) photoionization amplitudes which couple the bound-state density of the initial atom (ion) to many-electron scattering states with one electron in the continuum. Indeed, the derived final-state density matrix can be utilized to calculate all observable properties in the atomic photoionization process such as total cross sections, the alignment of the ions or the spin polarization of the photoelectrons. In Sec. II D, this is shown for the angular distribution of the photoelectrons which requires the knowledge of the bound-free transition amplitudes. In Sec. II E, we later recall the definition of the *concurrence* as a useful measure for the entanglement of any system which consists of two distinguishable qubits, while the computations of the transition amplitudes are briefly described in Sec. II F.

Although the main emphasis of this work concerns the setup of a proper formalism to consider the change of entanglement in atomic photoionization, which appears here as additional resource to the measurement of cross sections and angular distributions, Sec. III shows a few selected computations for the 5*s* valence-shell photoionization of neutral strontium near the ionization threshold. These calculations for the entanglement between the photoion and the emitted electron are based on amplitudes which are obtained in the framework of the multiconfiguration Dirac-Fock method. These results demonstrate that the entanglement is altered substantially, especially for photon energies near the ionization threshold, in dependence of the photon energy and angle. Finally, a brief summary is given in Sec. IV.

II. THEORY

A. Geometric setup

In order to describe the photoionization process, we shall first define proper coordinates to describe the photoionization of atoms and ions in full detail. In Fig. 1, a simplified geometrical setup is shown for the ionization of a single electron with well-defined asymptotic momentum $\boldsymbol{p}$. For the sake of convenience (which will become clear later), here we choose the quantization axis parallel to the electron momentum $\boldsymbol{p}$, in contrast to many previous investigations where the propagation direction of the incoming light was taken for the (spin-) quantization of the system. In the relativistic theory, in fact, the projection of the electron spin may have a sharp value only along the axis of the (electron) momentum. For this choice of the quantization axis, the direction $\hat{\boldsymbol{k}}$ of the incoming photon is characterized completely by the polar angle θ with respect to the outgoing electron.

B. Density-matrix formalism

Since the introduction of the density matrix by von Neumann and Landau in 1927, this formalism has been found to be a useful and elegant tool in many fields of modern physics. In atomic physics, for instance, the density matrix approach has been applied for studying the capture and emission of particles as well as the interaction of atoms with the radiation field and other processes [10–14].

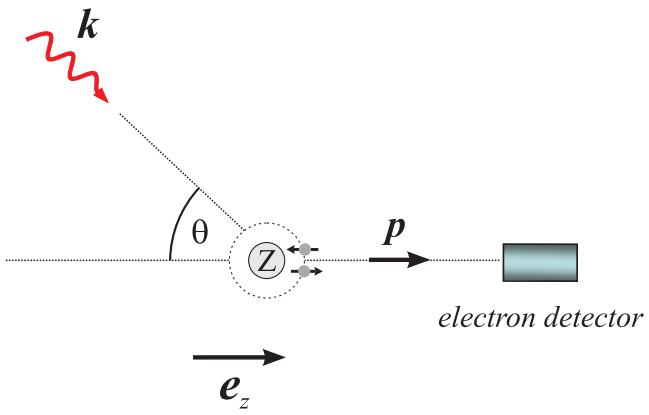

FIG. 1. (Color online) Geometry of the ionization process in which one valence shell electron of a trapped atom (or ion) is photoionized by a (circularly polarized) photon of energy $\hbar\omega$. Since the quantization axis is chosen parallel to the emitted electron, the incoming photon can be characterized by means of the (polar) angle θ with respect to this axis.

Instead of the explicit use of the density matrix, the state of a given system is often described in terms of the so-called statistical or density operator. This operator can be considered to represent an ensemble of identical physical systems which are altogether either in a pure state or in a statistical mixture of different (pure) states. The time-independent density matrix formalism is especially appropriate in order to describe the evolution of an initial system in passing through several interaction processes until the final state is attained. From the density matrix of this final state, then all the observable properties can be derived by using proper projections (traces).

In the following, we apply the density matrix theory to the photoionization of atoms and ions in a weak radiation field, i.e., if the absorption of a single photon leads to the emission of a photoelectron with well-defined momentum. The initial state of the overall system atom+radiation field therefore consists of the initial state of the atom as well as the representation of the incident photon. If both subsystems are initially uncorrelated (as always in usual photoionization experiments), then the initial-state density operator is given by the direct product of the density operators of the subsystems,

$$\hat{\rho}_i = \hat{\rho}_{\text{atom}} \otimes \hat{\rho}_{\text{photon}} = \hat{\rho}_0 \otimes \hat{\rho}_\gamma. \tag{1}$$

In addition, we assume below that the atom (ion) is described uniquely by a set α_0 of inner coordinates (quantum numbers) and the total angular momentum J_0 so that the initial state of the atom can be written as a general mixed state with respect to the spin projection M_0,

$$\hat{\rho}_0 = \sum_{M_0 M_0'} c_{M_0 M_0'} |\alpha_0 J_0 M_0\rangle\langle \alpha_0 J_0 M_0'|. \tag{2}$$

Similarly, we may specify also the spin state of the incident photon (beam) by the photon density matrix

$$\hat{\rho}_\gamma = \sum_{\lambda\lambda'} c_{\lambda\lambda'} |\boldsymbol{k}\lambda\rangle\langle\boldsymbol{k}\lambda'| \tag{3}$$

in the helicity representation, where λ is the spin projection of the photon onto the direction of its momentum $\hat{\boldsymbol{k}}$. Since for the photon (with intrinsic spin $S=1$) the helicity may take the values $\lambda=\pm 1$, only three independent parameters are required to describe the spin state of the photon by its 2×2 density matrix (3); they are closely related to the well-known Stokes parameters of light [11,12]

$$(c_{\lambda\lambda'}) = \langle\boldsymbol{k}\lambda|\hat{\rho}_\gamma|\boldsymbol{k}\lambda'\rangle = \frac{1}{2}\begin{pmatrix} 1+P_3 & P_1 - iP_2 \\ P_1 + iP_2 & 1-P_3 \end{pmatrix} \tag{4}$$

which, in optics and atomic physics, are often utilized to characterize the degree of the polarization of the light. While P_3 reflects the degree of circular polarization, the parameters P_1 and P_2 together denote the degree and direction of the linear polarization of the light in the plane perpendicular to the photon momentum $\boldsymbol{k}$.

As mentioned above, the density operator (1) describes the system atom+incoming photon in the initial state, i.e., before the photoionization has happened. In order to make use of this operator for the further analysis of the photoionization process, it is often more convenient to rewrite it in the matrix form

$$\langle\alpha_0 J_0 M_0, \boldsymbol{k}\lambda|\hat{\rho}_i|\alpha_0 J_0 M_0', \boldsymbol{k}\lambda'\rangle = c_{M_0 M_0'} c_{\lambda\lambda'}, \tag{5}$$

where we made use of the explicit representations (2) and (3). We can utilize this initial-state density matrix (5) to analyze the spin properties of the final system photoion +electron, following the photoinduced emission of an electron. These spin properties can be obtained from the final-state density operator $\hat{\rho}_f$ which, in turn, is related to $\hat{\rho}_i$ by the standard expression

$$\hat{\rho}_f = \hat{\mathcal{R}}\hat{\rho}_i\hat{\mathcal{R}}^\dagger. \tag{6}$$

In this relation, $\hat{\mathcal{R}}(\boldsymbol{k}) = \Sigma_i \boldsymbol{\alpha}_i \cdot \boldsymbol{u}_{\lambda,i} e^{i\boldsymbol{k}\cdot\boldsymbol{r}_i}$ is the transition operator which can be written as a sum of one-particle operators where each one-particle operator describes, within the framework of the relativistic Dirac theory, the interaction of the electron with the radiation field of the photon. Here, $\boldsymbol{\alpha}_i = (\alpha_{x,i}, \alpha_{y,i}, \alpha_{z,i})$ denotes the (vector of the) Dirac matrices and the unit vector $\boldsymbol{u}_{\lambda,i}$ specifies the circular polarization of the photon.

After the absorption of the photon, we have a *free* electron with asymptotic linear momentum $\boldsymbol{p}$ and spin projection m_s, while the photoion is left in a fine-structure state with total angular momentum J_f. Using a basis with well-defined (angular) momenta J_0 and J_f of the initial and the residual ion, the final-state density operator can be written as

$$\begin{aligned}
\langle\alpha_f J_f M_f, \boldsymbol{p} m_s|\hat{\rho}_f|\alpha_f J_f M_f', \boldsymbol{p} m_s'\rangle &= \sum_{M_0 M_0' \lambda\lambda'} \langle\alpha_f J_f M_f, \boldsymbol{p} m_s|\hat{\mathcal{R}}|\alpha_0 J_0 M_0, \boldsymbol{k}\lambda\rangle \\
&\quad \times \langle\alpha_0 J_0 M_0, \boldsymbol{k}\lambda|\hat{\rho}_i|\alpha_0 J_0 M_0', \boldsymbol{k}\lambda'\rangle\langle\alpha_0 J_0 M_0', \boldsymbol{k}\lambda'|\hat{\mathcal{R}}^\dagger|\alpha_f J_f M_f', \boldsymbol{p} m_s'\rangle \\
&= \sum_{M_0 M_0' \lambda\lambda'} c_{M_0 M_0'} c_{\lambda\lambda'} \left\langle \alpha_f J_f M_f, \boldsymbol{p} m_s \middle| \sum_i \boldsymbol{\alpha}_i \boldsymbol{u}_{\lambda,i} e^{i\boldsymbol{k}\cdot\boldsymbol{r}_i} \middle| \alpha_0 J_0 M_0 \right\rangle \\
&\quad \times \left\langle \alpha_f J_f M_f', \boldsymbol{p} m_s' \middle| \sum_i \boldsymbol{\alpha}_i \boldsymbol{u}_{\lambda',i} e^{i\boldsymbol{k}\cdot\boldsymbol{r}_i} \middle| \alpha_0 J_0 M_0' \right\rangle^*,
\end{aligned} \tag{7}$$

where $\langle\alpha_f J_f M_f, \boldsymbol{p} m_s|\Sigma_i \boldsymbol{\alpha}_i \cdot \boldsymbol{u}_{\lambda,i} e^{i\boldsymbol{k}\cdot\boldsymbol{r}_i}|\alpha_0 J_0 M_0\rangle$ represents the (photoionization) matrix element for the transition from a many-electron bound state of the atom to a scattering state with just one *free* electron in the continuum.

1. Partial wave and multipole expansion

For the computation and analysis of the final-state density matrix (7), further simplification of the transition amplitude $\langle\alpha_f J_f M_f, \boldsymbol{p} m_s|\Sigma_i \boldsymbol{\alpha}_i \cdot \boldsymbol{u}_{\lambda,i} e^{i\boldsymbol{k}\cdot\boldsymbol{r}_i}|\alpha_0 J_0 M_0\rangle$ is required. In order to achieve such a simplification we first must decompose the continuum wave function $|\boldsymbol{p} m_s\rangle$ of the emitted electron into partial waves. As discussed previously, special care must be taken in choosing the quantization axis since this influences the explicit form of the decomposition. For instance, using the electron momentum $\boldsymbol{p}$ as the quantization axis (cf. Fig. 1), the full expansion of the continuum wave function is given by [15]

$$|\boldsymbol{p} m_s\rangle = \sum_{\substack{\kappa=-\infty \\ (\kappa\neq 0)}}^{+\infty} i^l e^{i\Delta_\kappa} \sqrt{4\pi(2l+1)} \left(l 0 \frac{1}{2} m_s | j m_s \right) |\varepsilon\kappa j m_s\rangle, \tag{8}$$

where the summation runs over all values of Dirac's angular momentum quantum number

$$\kappa \equiv \kappa(j,l) = \pm(j+1/2) \quad \text{for } l = j \pm 1/2,$$

and ε denotes the kinetic energy of the ejected electron and j and $(-1)^l$ the total angular momentum and parity of the partial waves $|\varepsilon\kappa j m_s\rangle$. Moreover, the additional phase shift Δ_κ in Eq. (8) arises from the potential of the nucleus and the remaining electrons of the photoion.

Apart from the continuum wave function of the outgoing electron, we shall rewrite in a second and independent expansion also the one-particle operators of the transition operator $\hat{\mathcal{R}}(\hat{\boldsymbol{k}})$ in terms of spherical tensors, i.e., in terms of electric and magnetic multipole fields. Given the wave vector $\boldsymbol{k}$ of the ionizing photon, the multipole decomposition of the photon wave is defined by

$$\boldsymbol{u}_\lambda e^{i\boldsymbol{k}\cdot\boldsymbol{r}} = \sqrt{2\pi}\sum_{L=1}^{\infty}\sum_{M=-L}^{+L} i^L\sqrt{2L+1}\mathcal{A}^{(\lambda)}_{LM}D^L_{M\lambda}(\hat{\boldsymbol{n}}), \tag{9}$$

where

$$\mathcal{A}^{(\lambda)}_{LM} = \mathcal{A}^{(m)}_{LM} + i\lambda\mathcal{A}^{(e)}_{LM} = \sum_{p=0,1}(i\lambda)^p\mathcal{A}^{(p)}_{LM} \tag{10}$$

represent the magnetic ($p=0$) and electric ($p=1$) multipole fields and $D^L_{M\lambda}(\hat{\boldsymbol{n}})=D^L_{M\lambda}(\boldsymbol{k}\rightarrow\boldsymbol{e}_z)$ is the Wigner D-function or Wigner rotation matrix of rank L. This matrix takes into account the fact that we have chosen the direction of the electron momentum $\boldsymbol{p}$ as the quantization instead of the photon momentum $\boldsymbol{k}$.

2. Derivation of the final-state matrix elements

Inserting the partial wave expansion Eq. (8) for the continuum wave of the free electron and the multipole expansion Eqs. (9) and (10) of the photon field into Eq. (7), the final-state spin density matrix can be written (up to some normalization constant) as

$$\begin{aligned}\langle\alpha_f J_f M_f,\boldsymbol{p}m_s|\hat{\rho}_f|\alpha_f J_f M'_f,\boldsymbol{p}m'_s\rangle = &\sum_{\substack{M_0M'_0\lambda\lambda' pp'\\ LL'MM'\kappa\kappa'}} c_{M_0M'_0}c_{\lambda\lambda'}i^{-l+l'+L-L'}(i\lambda)^p(i\lambda')^{p'}\\ &\times e^{i(\Delta_\kappa-\Delta_{\kappa'})}[l,l',L,L']^{1/2}\left\langle l0\frac{1}{2}m_s|jm_s\right\rangle\left\langle l'0\frac{1}{2}m'_s|j'm'_s\right\rangle\left\langle\alpha_f J_f M_f;\varepsilon\kappa jm_s\left|\sum_i\boldsymbol{\alpha}_i\mathcal{A}^{(p)}_{LM,i}\right|\alpha_0J_0M_0\right\rangle\\ &\times\left\langle\alpha_f J_f M'_f;\varepsilon\kappa' j'm'_s\left|\sum_i\boldsymbol{\alpha}_i\mathcal{A}^{(p')}_{L'M',i}\right|\alpha_0J_0M'_0\right\rangle^* D^L_{M\lambda}(\hat{\boldsymbol{n}})D^{L'^*}_{M'\lambda'}(\hat{\boldsymbol{n}}),\end{aligned} \tag{11}$$

where we used the notation $[l,l',\ldots]=(2l+1)(2l'+1)\ldots$.

Indeed, Eq. (11) represents the most general form of the final-state density which describes the spin states of both the emitted photoelectron $|\boldsymbol{p}m_s\rangle$ and the residual ion $|\alpha_f J_f M_f\rangle$. In this form, all wave functions and operators (in the transition matrix elements) are now expressed in a *spherical representation* and can thus be evaluated by using the techniques of Racah's algebra [16]. To construct the many-electron scattering states of well-defined symmetry, we may use the standard procedure for the coupling of the angular momenta $\boldsymbol{J}_f$ and $\boldsymbol{j}$ of the residual ion and the ejected electron

$$|\alpha_f J_f M_f;\varepsilon\kappa jm_s\rangle = \hat{A}\sum_{J_tM_t}(J_fM_fjm_s|J_tM_t)|(\alpha_fJ_f,\kappa):J_tM_t\rangle, \tag{12}$$

where the operator $\hat{A}$ is used to ensure the proper antisymmetrization of the emitted photoelectron with respect to the bound-state wave function. Inserting the expression (12) into Eq. (11), the final-state density matrix can be rewritten as

$$\begin{aligned}\langle\alpha_f J_f M_f,\boldsymbol{p}m_s|\hat{\rho}_f|\alpha_f J_f M'_f,\boldsymbol{p}m'_s\rangle = &\sum_{\substack{M_0M'_0\lambda\lambda' pp'\\ LL'MM'\kappa\kappa'}}\sum_{\substack{J_tM_t\\ J'_tM'_t}} c_{M_0M'_0}c_{\lambda\lambda'}(i\lambda)^p(i\lambda')^{p'}i^{-l+l'+L-L'}\\ &\times e^{i(\Delta_\kappa-\Delta_{\kappa'})}[l,l',L,L']^{1/2}(l01/2m_s|jm_s)(l'01/2m'_s|j'm'_s)(J_fM_fjm_s|J_tM_t)(J_fM'_fj'm'_s|J'_tM'_t)\\ &\times\left\langle(\alpha_fJ_f,\kappa):J_tM_t\left|\sum_i\boldsymbol{\alpha}_i\mathcal{A}^{(p)}_{LM,i}\right|\alpha_0J_0M_0\right\rangle\\ &\times\left\langle(\alpha_fJ_f,\kappa'):J'_tM'_t\left|\sum_i\boldsymbol{\alpha}_i\mathcal{A}^{(p')}_{L'M',i}\right|\alpha_0J_0M'_0\right\rangle^* D^L_{M\lambda}(\hat{\boldsymbol{n}})D^{L'^*}_{M'\lambda'}(\hat{\boldsymbol{n}}),\end{aligned} \tag{13}$$

where $M_t = M_f + m_s$ and $M'_t = M'_f + m'_s$.

We are now prepared to make a last step in evaluating the final-state density matrix and bring it into the form which is most convenient for computations. By making use of the Wigner-Eckart theorem

$$\left\langle (\alpha_f J_f, \kappa) : J_t M_t \left| \sum_i \boldsymbol{\alpha}_i \mathcal{A}^{(p)}_{LM,i} \right| \alpha_0 J_0 M_0 \right\rangle = \frac{1}{\sqrt{2J_t+1}} (J_0 M_0 LM | J_t M_t) \times \left\langle (\alpha_f J_f, \varepsilon\kappa j), J_t \left\| \sum_i \boldsymbol{\alpha}_i \mathcal{A}^{(p)}_{L,i} \right\| \alpha_0 J_0 \right\rangle \quad (14)$$

and introducing the short-hand notation

$$\langle (\alpha_f J_f, \varepsilon\kappa j), J_t \| H_{Lp} \| \alpha_0 J_0 \rangle = i^{-l} e^{i\Delta_\kappa} \left\langle (\alpha_f J_f, \varepsilon\kappa j), J_t \left\| \sum_i \boldsymbol{\alpha}_i \mathcal{A}^{(p)}_{L,i} \right\| \alpha_0 J_0 \right\rangle, \quad (15)$$

we are able to trace back the final-state density matrix elements to the reduced matrix elements of the multipole fields. These reduced matrix elements form the fundamental building blocks for the evaluation of a large number of properties related to the atomic photoionization process and have been discussed in detail in Ref. [13]. Inserting Eqs. (14) and (15) into (13) we finally obtain a rather general expression for the final-state density matrix which describes the overall system photoion+electron following the photoionization process:

$$\langle \alpha_f J_f M_f, \boldsymbol{p} m_s | \hat{\rho}_f | \alpha_f J_f M'_f, \boldsymbol{p} m'_s \rangle = \sum_{\substack{M_0 M'_0 \lambda\lambda' pp' \\ LL' MM' \kappa\kappa'}} \sum_{\substack{J_t M_t \\ J'_t M'_t}} c_{M_0 M'_0} c_{\lambda\lambda'} i^{L-L'} \frac{[l,l',L,L']^{1/2}}{[J_t, J'_t]^{1/2}} \times (l01/2 m_s | jm_s)(l'01/2 m'_s | j' m'_s)(J_f M_f jm_s | J_t M_t)(J_f M'_f j' m'_s | J'_t M'_t)(J_0 M_0 LM | J_t M_t) \times (J_0 M'_0 L' M' | J'_t M'_t) \langle (\alpha_f J_f, \varepsilon\kappa j), J_t \| H_{Lp} \| \alpha_0 J_0 \rangle \langle (\alpha_f J_f, \varepsilon\kappa' j'), J'_t \| H_{L'p'} \| \alpha_0 J_0 \rangle^* D^L_{M\lambda}(\hat{\boldsymbol{n}}) D^{L'*}_{M'\lambda'}(\hat{\boldsymbol{n}}). \quad (16)$$

The theory developed so far is general and not restricted to any shell structure of the initial atom or the photoionization of an electron from a particular shell. Formula (16) applies even for the case that the photoinduced emission of an electron is accompanied by the excitation or shake-up of other bound-state electrons, leading to some satellite lines in the photoelectron spectrum. However, in order to interpret the spin states of the residual photoion and the ejected electron as two distinguishable quantum bits (*qubits*), i.e., as two-state systems in both cases, it is useful to restrict the further analysis to the photoionization of a (closed-shell) atom in a $ns^2\ ^1S_0$ ground state. Such a configuration applies, for instance, for all alkaline-earth metal atoms and their isoelectronic sequences. For any $^1S_0$ initial state, we may suppose the atom to be maximally entangled as a consequence of the Pauli principle. Note, however, that the *concurrence* (cf. Sec. II E) cannot be used for measuring the entanglement of the system, as this measure assumes two distinguishable subsystems. If, moreover, we consider the direct photoionization of one of the *ns* electrons, the photoion is left in a stable $ns\ ^2S_{1/2}$ ground state ($J_f = 1/2$) of the singly ionized atom. Obviously, this restriction allows for an immediate interpretation of the total system photoion+electron as a two-qubit system whose entanglement can be characterized by means of the concurrence measure. Other quantum measures might be used to characterize and analyze the entanglement also for photoionization processes which result in final states of the photoion with $J_f > 1/2$, i.e., in arbitrary $d_1 \times d_2$ quantum systems [17,18]. A further interesting scenario for studying the entanglement transfer in the course of atomic photoionization occurs if inner-shell hole states are created which decay by photon or electron emission. In this case, the treatment of the photoionization must be extended considerably to incorporate the intermediate resonance states (of the photoion) in the setup and computations of the final-state density matrix.

C. Photoionization with unpolarized or circularly polarized light

Formula (16) for the final-state density matrix can be further simplified if, other than unpolarized atoms in their initial state, we consider the photoionization by unpolarized or circularly polarized light. In this case, the density operators of the atom and photon [cf. Eqs. (2) and (3)] become

$$\hat{\rho}_0 = \frac{1}{2J_0+1} \sum_{M_0} |\alpha_0 J_0 M_0\rangle\langle \alpha_0 J_0 M_0| \quad (17)$$

and

$$\hat{\rho}_\gamma = \sum_\lambda c_{\lambda\lambda} |\boldsymbol{k}\lambda\rangle\langle\boldsymbol{k}\lambda|, \tag{18}$$

where $c_{\lambda\lambda}=1/2$ applies for the case of unpolarized light while $c_{\lambda\lambda}=\delta_{\lambda,\pm 1}$ describes the left ($\lambda=-1$) and the right ($\lambda=+1$) circularly polarized light. The combined initial-state matrix elements (5) thus simplify to

$$\langle \alpha_0 J_0 M_0, \boldsymbol{k}\lambda | \hat{\rho}_i | \alpha_0 J_0 M_0', \boldsymbol{k}\lambda' \rangle = \delta_{\lambda\lambda'} \delta_{M_0 M_0'} \frac{c_{\lambda\lambda}}{2J_0+1}. \tag{19}$$

Inserting Eq. (19) into expression (16) and by making use of Racah's algebra, the final-state density matrix for unpolarized or circularly polarized light becomes

$$\begin{aligned}\langle \alpha_f J_f M_f, \boldsymbol{p} m_s | \hat{\rho}_f | \alpha_f J_f M_f', \boldsymbol{p} m_s' \rangle = & \sum_{\substack{\nu\mu LL' \\ \lambda\kappa\kappa'}} \sum_{\substack{J_t M_t \\ J_t' M_t'}} c_{\lambda\lambda} D^\nu_{\mu 0}(0,\theta,0) i^{L-L'} \frac{[l,l',L,L',\nu]^{1/2}}{[J_t]^{1/2}} \\ & \times (-1)^{J_0+J_t'+1} (l 0 1/2 m_s | j m_s)(l' 0 1/2 m_s' | j' m_s') \\ & \times (J_f M_f j m_s | J_t M_t)(J_f M_f' j' m_s' | J_t' M_t')(\nu\mu J_t' M_t' | J_t M_t)(L\lambda L' -\lambda | \nu 0) \begin{Bmatrix} L' & L & \nu \\ J_t & J_t' & J_0 \end{Bmatrix} \\ & \times \langle (\alpha_f J_f, \varepsilon\kappa j), J_t \| H_L \| \alpha_0 J_0 \rangle \langle (\alpha_f J_f, \varepsilon\kappa' j'), J_t' \| H_{L'} \| \alpha_0 J_0 \rangle^*, \end{aligned} \tag{20}$$

where $\{\cdots\}$ denotes the Wigner $6j$ symbol and where the summation over ν is restricted by $\nu=|L-L'|,\ldots,L+L'$. In Eq. (20), moreover, we used the fact that for unpolarized or circularly polarized light, the rotation $\boldsymbol{k}\to\boldsymbol{e}_z$ of the photon wave is completely characterized by a single angle θ so that $D^\nu_{\mu 0}(\hat{\boldsymbol{n}})=D^\nu_{\mu 0}(0,\theta,0)$.

D. Angular distribution of the photoelectrons

The final-state density matrix (20) contains the complete information about the system photoion+electron and, hence, can be utilized to derive all *observables* for both particles. In the density matrix theory, a (so-called) detector operator $\hat{P}$ can be assigned to each observable which projects out the (subspace of) final states leading to a click at the detectors in the present setup of the experiment. This detector operator also determines the probability W of registering an event at the detector simply by taking the trace of its product with the final-state density matrix $W=\mathrm{Tr}(\hat{P}\hat{\rho}_f)$.

For instance, to measure the angular distribution of the emitted photoelectrons, one usually applies a detector which is not sensitive to neither the spin of the photoelectron nor to the spin state of the residual ion,

$$\hat{P} = \sum_{M_f m_s} |\alpha_f J_f M_f, \boldsymbol{p} m_s\rangle\langle \alpha_f J_f M_f, \boldsymbol{p} m_s|, \tag{21}$$

as seen from the sum over the spin projections m_s of the electron and the magnetic quantum numbers M_f of the photoion. From this operator, we immediately obtain also the well-known angular distribution of the photoelectrons

$$W(\theta) = \mathrm{Tr}(\hat{\rho}_f) = \sum_{M_f m_s} \langle \alpha_f J_f M_f, \boldsymbol{p} m_s | \hat{\rho}_f | \alpha_f J_f M_f, \boldsymbol{p} m_s \rangle, \tag{22}$$

which is just the normal trace of the final-state density matrix.

E. Final-state entanglement

From the final-state density matrix (20) for the photoionization of an atom by unpolarized or (purely) circular polarized light, we can derive not only the individual properties of the outgoing electron or the residual ion but also those properties which are associated with the combined system photoion+electron. Apart from the outcome of various coincidence measurements, we may consider, for example, the quantum mechanical correlation of the (spins of the) two particles, i.e., their *spin entanglement*. Of course, in order to quantify this entanglement and to introduce a proper *measure* for it, information is first required about the possible spin states of each subsystem. Following the (direct) photoionization of a single electron, the electron and photoion are distinguishable eventually and can be treated as a two-qubit system with the four-dimensional product basis $\{|\uparrow\uparrow\rangle,|\uparrow\downarrow\rangle,|\downarrow\uparrow\rangle,|\downarrow\downarrow\rangle\}$, iff the residual ion has total angular momentum $J=1/2$ with $M_J=\pm 1/2$. This requirement is fulfilled, for instance, for the photoionization of a *ns* valence electron of alkaline-earth atoms, by starting from the (closed-shell) $ns^2\ ^1S_0$ ground state of the atoms (or isoelectronic ions) and leading to a photoion in a $ns\ ^2S_{1/2}$ ground level.

In general, the quantification of entanglement is still an unsolved problem for multipartite quantum systems if they are in a mixed state. For such systems, the possible entanglement measures are often defined as variational expressions which usually involve an optimization over all possible pure-

state decompositions $\rho=\Sigma_i p_i|\psi_i\rangle\langle\psi_i|$ of a mixed state ρ. For bipartite systems, such as described above for the photoinduced emission of a single electron, in contrast, several computable entanglement measures have been proposed during the last years (see, e.g., Ref. [19] for a recent introduction and review). For two-qubit systems, the so-called *concurrence* is certainly the most widely used measure [20,21]. For an arbitrary two-qubit state, either pure or mixed, described by the density operator $\hat{\rho}$, the concurrence is defined as

$$\mathcal{C}(\hat{\rho}) = \max(0, \sqrt{\lambda_1} - \sqrt{\lambda_2} - \sqrt{\lambda_3} - \sqrt{\lambda_4}), \tag{23}$$

where $\sqrt{\lambda_i}$ are the square roots of the eigenvalues (i.e., the singular values) of the matrix $\tilde{\hat{\rho}}\hat{\rho}$ in descending order and where $\tilde{\hat{\rho}}$ denotes the so-called spin-flipped matrix,

$$\tilde{\hat{\rho}} \equiv (\hat{\sigma}_y^{(1)} \otimes \hat{\sigma}_y^{(2)})\hat{\rho}^*(\hat{\sigma}_y^{(1)} \otimes \hat{\sigma}_y^{(2)}). \tag{24}$$

In the definition (24) of the spin-flipped matrix, $\hat{\rho}^*$ refers to the complex conjugate of $\hat{\rho}$, and $\hat{\sigma}_y^{(1)}$ and $\hat{\sigma}_y^{(2)}$ are the standard Pauli matrices acting on the first and the second qubit, respectively.

Using the formulas (23) and (24), we are able to determine the degree of entanglement from the final-state density matrix (16) or (20) if it represents a proper two-qubit system. All that is needed is to ensure that the two subsystems photoion+electron can be treated as distinguishable two-state systems on which (projetive) measurements can be carried out. In Sec. III, these formulas are applied for studying the concurrence between the photoion and the ejected electron following the $5s$ photoionization of neutral strontium. The computations of the final-state concurrence have been performed using the FEYNMAN program which has been developed in our group for the simulation and (entanglement) analysis of quantum registers [22].

F. Computations

Our discussion above shows how the computation of the density matrix and, hence, of most properties in the photoionization of atoms and ions can be traced back to the reduced matrix elements (15) which describe the interaction of an electronic bound state with the radiation field. Since these reduced matrix elements occur very frequently in the calculation of atomic data, such as transition probabilities and ionization cross sections, here we do not need to discuss their evaluation in detail. In the computations below, we applied the (relativistic) multiconfiguration Dirac-Fock method to approximate proper bound-state wave functions and for evaluating all the required matrix elements. The calculations were carried out by means of the RATIP program of our group [23,24] which now provides also the (reduced) photoionization amplitudes (15) for atoms and ions in rather arbitrary configurations [25,26].

The MCDF method has been found useful in many atomic calculations, especially for medium and heavy elements or if (several) open shells are involved. Not much needs to be said here about this method [23,27], in which an atomic state is approximated by a linear combination of (so-called) configuration state functions (CSFs) of the same symmetry

$$\psi_\alpha(PJM) = \sum_{r=1}^{n_c} c_r(\alpha)|\gamma_r PJM\rangle. \tag{25}$$

In this ansatz for an atomic state, n_c is the number of CSF and $\{c_r(\alpha)\}$ denotes its representation in this basis. In most computations, moreover, the CSF are constructed as antisymmetrized products of a common set of orthonormal orbitals and are optimized on the basis of the Dirac-Coulomb Hamiltonian. Further relativistic contributions to the representation $\{c_r(\alpha)\}$ of the atomic states are then added, owing to the given requirements, by diagonalizing the Dirac-Coulomb-Breit Hamiltonian matrix in first-order perturbation theory.

Besides the reduced matrix elements

$$\langle(\alpha_f J_f, \varepsilon\kappa j), J_t\|H_{Lp}\|\alpha_0 J_0\rangle$$

as the key ingredients for calculating the final-state density matrix, Eq. (16) also displays the *angular part* of the density matrix which consists of the six Clebsch-Gordan coefficients and some phase factors. Owing to the 16-fold summation in Eq. (16), special care must be taken to achieve an efficient evaluation of these coefficients. Below, we made use of the RACAH [28] and DIRAC [29] programs which have been developed in our group in Kassel for dealing with the atomic shell model.

III. RESULTS AND DISCUSSION

Section II describes how the density matrix theory can be utilized in order to discuss and analyze the change (and control) of entanglement in the photoionization of many-electron atoms and ions. Equations (16) and (20) for the final-state density matrix of the system photoion+electron, in particular, are the main result of this work which can be applied immediately for studying various ionization processes; they show how atomic photoionization can provide an alternative path in creating entanglement (of given degree) in atomic systems. As a first example, let us consider here the photoionization of neutral strontium ($Z=38$), starting from its singlet ground state $\psi=[\mathrm{Kr}]5s^2\ {}^1S_0$. Owing to Pauli's principle, this state can be considered as completely spin-entangled although this property is not required for analyzing the entanglement between the photoion and the outgoing electron after the photoionization has occurred. Therefore, we shall not discuss whether and how this *initial* entanglement of the (bound electrons of an) atom could be specified quantitatively by means of a mathematically sound measure; as in Ref. [8], we simply define $\mathcal{C}(\hat{\rho}_0)=1$.

After the emission of one of the $5s$ valence electrons owing to the absorption of either right-circular ($\lambda=+1$) or unpolarized light:

$$\mathrm{Sr} + h\nu \rightarrow \mathrm{Sr}^+(5s^2 S_{1/2}) + e^-,$$

the spin entanglement between the singly ionized Sr^+ ion in its $[\mathrm{Kr}]\ 5s\ {}^2S_{1/2}$ ground state and the ejected photoelectron is determined by the final-state density matrix (20). Apart from the internal structure of the strontium atom, this density matrix depends also on the energy E_γ as well as the direction θ and the polarization of the incident light (cf. Fig. 1). In the

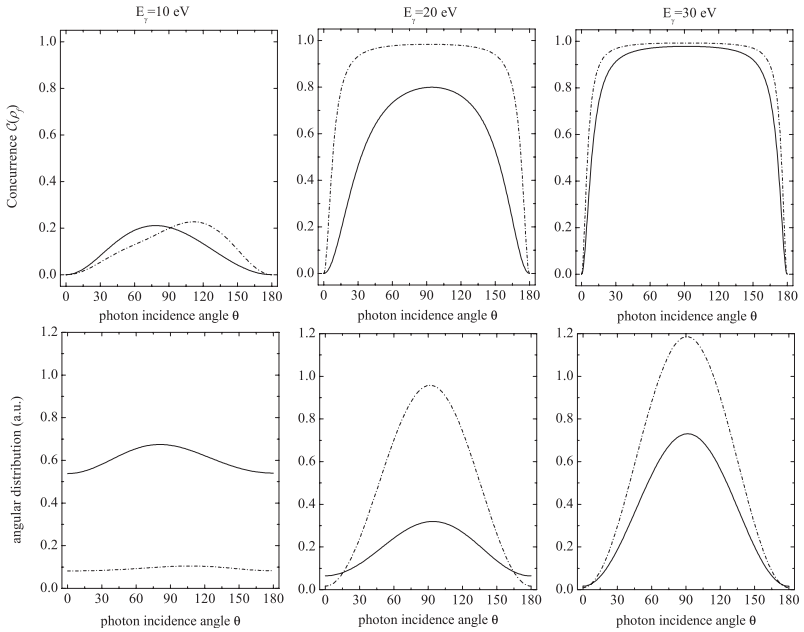

FIG. 2. (Upper panel) Final-state concurrence value as a function of the photon incidence angle θ. Results are shown for the case of right-circularly polarized light and for different photon energies $E_1=10$ eV, $E_2=20$ eV, $E_3=30$ eV as well as for length gauge (—) and velocity gauge (---). (Lower panel) Angular distribution of the photoelectrons using length gauge (—) and velocity gauge (---).

following, we calculate the concurrence of this two-qubit system above and investigate how it depends on these parameters. Having once understood this dependence, of course, we may reverse our argumentation above and use the photoionization process in order to extract photoion-electron pairs with a given degree of entanglement.

For the $5s$ photoionization of atomic strontium, Fig. 2 (upper panel) displays the concurrence of the final Sr^+ ion-electron pair as a function of the photon angle θ. Results are shown for right-circular light in length and velocity gauge and for the three photon energies $E_\gamma=10$ eV, 20 eV, and 30 eV, respectively. When compared to the initial concurrence of $\mathcal{C}(\hat{\rho}_0)=1$, a strong decrease occurs in forward and backward direction of the incoming photons as well as if one approaches the photoionization threshold at $E_{\mathrm{thr}}=5.69$ eV. The rather large changes in the degree of entanglement between the photoion and the outgoing electron reflects the electron-electron and spin-orbit interaction in the ground state of strontium and will be discussed below.

Of course, in order to measure the concurrence of a photoion-electron pair for a given angle θ of the incident photon beam, we would need enough intensity for the emission of an electron under these circumstances. In the lower panel of Fig. 2, therefore, we also display the angular distribution for right-circularly polarized light and at the same photon energies as above. As seen from this figure, the angular distribution is mainly proportional to $(\sin\theta)^2$ which is well known from the emission pattern of the s-shell photoionization in the nonrelativistic regime. In particular, it can be seen that the electron emission occurs mainly perpendicular to the direction of the incoming light ($\theta=90°$) while the forward and backward emission is strongly suppressed.

Note however that near to the ionization threshold, i.e., for $E_\gamma \lessapprox 10$ eV, the photoionization amplitudes occur to be very sensitive to correlation effects. This is seen, for instance, from the rather large deviations in the angular distributions if they are calculated in the two different couplings of the radiation field to the bound state density, namely in length and velocity gauge. These deviations between the two gauges arise partially from the fact that rather restricted wave-function expansions (25) have been used for both initial and final ionic states. A better agreement between the gauges might be expected if the number of correlation state functions is increased. This would lead, however, also to a significant increase in the computational requirements which does not seem to be necessary for the qualitative discussion in the present work.

In contrast to the angular distribution, the concurrence (i.e., the degree of entanglement) between the photoion and the electron appears less sensitive with regard to the gauge form for the coupling of the radiation field. As seen from the upper panel of Fig. 2, the discrepancy between length and velocity gauge is for $\theta=90°$ about 20% at $E_\gamma=20$ eV and decreases to 3% for $E_\gamma \geqslant 30$ eV (including those energies which are not shown in this figure). Apart from low photon energies, the concurrence follows the symmetry of the angular distributions of the photoelectrons; in particular, it appears symmetric with respect to a forward ($\theta<90°$) and backward emission ($\theta>90°$) of the ejected electron. As discussed above, this symmetry might occur even for low photon energies $E_\gamma=10$ eV, for which, however, the accuracy in calculating the reduced photoionization amplitudes (15) is not high enough to interpret the different shapes of the concurrence in the two gauges from above.

While the shape of the concurrence, considered as a function of the photon angle, is quite independent of the energy of the incoming light, the absolute values $\mathcal{C}(\hat{\rho}_f)$ for $E_\gamma=10$ eV decreases to a maximum value $\mathcal{C}(\hat{\rho}_f)\approx 0.2$ which shows that most of the initial entanglement $\mathcal{C}(\hat{\rho}_0)=1$ is lost in the course of the photoabsorption and simultaneous electron

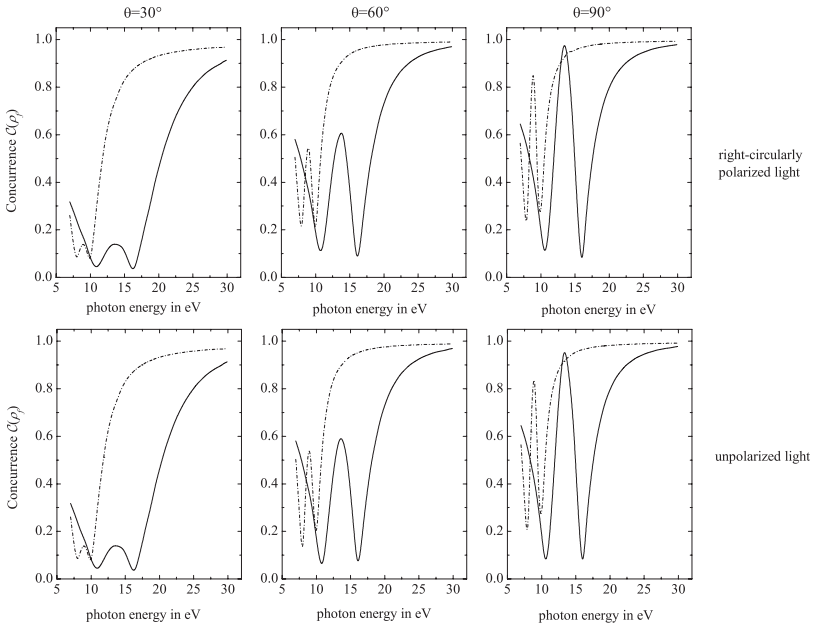

FIG. 3. Final-state concurrence as a function of the photon energy for fixed photon angles $\theta=30°$, $\theta=60°$, and $\theta=90°$ as well as for right-circularly polarized light (upper panel) and unpolarized light (lower panel). Results are shown for length gauge (—) and velocity gauge (-·-).

emission. This strong decrease of the entanglement near the photoionization threshold must be attributed to many-particle and spin-orbit effects, which are dominant in the low-energy regime [30]. For higher photon energies, in contrast, these effects become less important leading to a concurrence $\mathcal{C}(\hat{\rho}_f) \lessapprox 1$ over a wide range of angles. This conservation of the concurrence, when compared to $\mathcal{C}(\hat{\rho}_0)=1$, also follows from the properties of the electron-photon interaction: The transition operator $\hat{\mathcal{R}}(\boldsymbol{k})=\Sigma_i \boldsymbol{\alpha}_i \cdot \boldsymbol{u}_{\lambda,i} e^{i\boldsymbol{k}\cdot\boldsymbol{r}_i}$ itself is independent of the spin coordinates, at least within the nonrelativistic limit, and hence cannot directly affect the spin of the electrons. For the photon energies $E_\gamma=20$ and 30 eV, the angular distribution of the concurrence $\mathcal{C}(\hat{\rho}_f)$ approaches the shape which was obtained before within the IPM where the initial entanglement is fully preserved for all angles except for $\theta \to 0°$ and $\theta \to 180°$ [8,9].

Until now we have discussed the angular distribution of the final-state concurrence for fixed energies of the incoming photon. Figure 3 displays in addition the energy dependence of the concurrence for the three photon angles $\theta=30°$, 60°, and 90°. These angles of the incident photons have been chosen since the electron emission is predominant in the angle range of $30° \leqslant \theta \leqslant 90°$ (cf. bottom panel of Fig. 2). Again, the concurrence $\mathcal{C}(\hat{\rho}_f)$ is shown in length and velocity gauge to document the sensitivity of this measure with respect to the way we treat the coupling of the radiation field to the bound-state electron density in the many-electron computations. As seen from the upper panel in Fig. 3, both gauges yield qualitatively similar results. For all three photon angles, a significantly reduced entanglement of $\mathcal{C}=0.3-0.6$ is found near the ionization threshold $E_{\mathrm{thr}}=5.69$ eV. An even smaller degree of entanglement can be found around the two well-pronounced minima at $E_\gamma \approx 11$ eV (8 eV) and $E_\gamma \approx 16$ eV (10 eV) for length (velocity) gauge. The positions of these two minima are largely independent of the photon angle. Finally, for $E_\gamma > 17$ eV, the concurrence rapidly approaches unity as it should be expected since the independent particle model becomes a good approximation again when the photon energy is (much) larger than the interelectronic and spin-orbit interactions.

Although the energy dependence of the final-state concurrence is quite similar for the three angles of the incoming light, the absolute values of $\mathcal{C}(\hat{\rho}_f)$ do depend on the particular choice of θ. For instance, the value of the concurrence maximum near $E_\gamma=14$ eV strongly depends on the photon angle and increases from $\mathcal{C} \approx 0.15$ at $\theta=30°$ up to $\mathcal{C} \approx 0.97$ at $\theta=90°$ (length gauge).

Up to the present, all results for the angular and energy dependence of the concurrence between the spins of the photoelectron and the residual Sr^+ ($5s\ ^2S_{1/2}$) ion were shown for the case of right-circularly polarized light. In order to explore the dependence of the final-state concurrence on the polarization of the incoming light, calculations have been performed also for the photoionization of neutral strontium by unpolarized light. As seen from the lower panel of Fig. 3, the concurrence is hardly affected by the (circular) polarization of the incoming light. A stronger effect may be expected for the case of linearly polarized light which is however not included in the formalism presented above. Compared to the special-case simplifications in Sec. II C, the investigation of linear polarization effects would require a more complicated geometry including the introduction of an additional angle for describing the polarization plane's orientation.

IV. SUMMARY AND OUTLOOK

The density matrix theory has been applied for studying the entanglement between the photoelectron and residual ion

in the course of the photoionization of atoms and ions. This generalizes our previous work in Ref. [9] for many-electron atoms, by including interelectronic effects and the higher multipoles of the radiation field. Emphasis has been placed on deriving the final-state density matrix of the photoelectron *and* the residual ion which enables one to analyze the change of entanglement (concurrence) as a function of the energy, angle and the polarization of the incoming light.

In a first application of this theory, we calculated the photoion-electron entanglement for the $5s$ photoionization of neutral strontium with a $5s^2\ ^1S_0$ ground state, leading to a photoion in a $5s\ ^2S_{1/2}$ state, i.e., in a $J_f=1/2$ level. After the emission of the electron, therefore, the final system photoion+electron can be considered as a (distinguishable) two-qubit system for which the concurrence provides a measure for the degree of entanglement. The concurrence of this system has been calculated as function of the angle and energy of the photons as well as for right-circularly polarized and unpolarized light. From these calculations, it is found that the initial-state entanglement [which is assumed to be $\mathcal{C}(\hat{\rho}_0)=1$ for the $^1S_0$ ground state of strontium] decreases significantly near the photoionization threshold and, in general, depends on both, the photon energy and angle. On the other hand, our results do not show any notable influence of the final-state entanglement on the photon polarization. For photon energies $E_\gamma > 20$ eV, the initial-state entanglement is almost fully preserved which agrees with results obtained within the independent particle model [8,9]. Note, however, that for these energies the $4p$ photoelectron emission starts to dominate the photoionization of neutral strontium, leading to resonance phenomena in the cross sections [25,31] and the emission of (additional) Auger electrons.

Knowledge about the entanglement between the photoelectron and the residual ion provides an *alternative view* on the fundamental process of atomic photoionization which comes in addition to the study of (photoionization) cross sections, angular distributions, or the spin-polarization of the outgoing electron. While the latter three properties are associated with either the photoion or the electron, the entanglement between these particle is a property of both. Moreover, a detailed understanding of the (change of) entanglement in the course of the photoionization, taken as functions of the various parameters of the incoming light, will enable one to extract photoion-electron pairs with a well-defined degree of entanglement. Such a control of the creation of entangled pairs may have far-reaching consequences not only in quantum information but also at several places elsewhere.

ACKNOWLEDGMENTS

This work has been supported by the DFG and the GSI under the Contract No. KS-FRT.

[1] A. Einstein, B. Podolsky, and N. Rosen, Phys. Rev. **47**, 777 (1935).
[2] E. Schrödinger, Proc. Cambridge Philos. Soc. **31**, 555 (1935); **32**, 446 (1936).
[3] M. A. Nielsen and I. L. Chuang, *Quantum Computation and Quantum Information* (Cambridge University Press, Cambridge, 2000).
[4] C. H. Bennett and S. J. Wiesner, Phys. Rev. Lett. **69**, 2881 (1992).
[5] A. K. Ekert, Phys. Rev. Lett. **67**, 661 (1991).
[6] P. W. Shor, in *Proceedings of the 35th Annual Symposium on the Foundations of Computer Science*, edited by S. Goldwasser (IEEE Computer Society, Los Alamitos, CA, 1994), p. 124; SIAM (Soc. Ind. Appl. Math.) J. Sci. Stat. Comput. **26**, 1484 (1997).
[7] L. K. Grover, Phys. Rev. Lett. **79**, 325 (1997).
[8] Y. S. Kim, Y. J. Kim, and R. H. Pratt, Phys. Scr., T **T110**, 79 (2004).
[9] T. Radtke, S. Fritzsche, and A. Surzhykov, Phys. Lett. A **347**, 73 (2005).
[10] K.-N. Huang, Phys. Rev. A **22**, 223 (1980).
[11] V. V. Balashov, A. N. Grum-Grzhimailo, and N. M. Kabachnik, *Polarization and Correlation Phenomena in Atomic Collisions* (Kluwer Academic Plenum, New York, 2000).
[12] K. Blum, *Density Matrix Theory and Applications*, 2nd ed. (Plenum, New York, 1996).
[13] S. Fritzsche, A. Surzhykov, and T. Stöhlker, Phys. Rev. A **72**, 012704 (2005).
[14] A. Surzhykov, U. D. Jentschura, T. Stöhlker, and S. Fritzsche, Phys. Rev. A **73**, 032716 (2006).
[15] J. Eichler and W. Meyerhof, *Relativistic Atomic Collisions* (Academic, San Diego, 1995).
[16] G. Racah, Phys. Rev. **61**, 186 (1941); **62**, 438 (1942); **63**, 367 (1943).
[17] P. Rungta, V. Bužek, C. M. Caves, M. Hillery, and G. J. Milburn, Phys. Rev. A **64**, 042315 (2001).
[18] K. Chen, S. Albeverio, and S.-M. Fei, Phys. Rev. Lett. **95**, 040504 (2005).
[19] M. B. Plenio and S. Virmani, e-print quant-ph/0504163.
[20] W. K. Wootters, Phys. Rev. Lett. **80**, 2245 (1998).
[21] W. K. Wootters, Quantum Inf. Comput. **1**, 27 (2001).
[22] T. Radtke and S. Fritzsche, Comput. Phys. Commun. **173**, 91 (2005); **175**, 145 (2006).
[23] S. Fritzsche, Phys. Scr., T **T100**, 37 (2002).
[24] S. Fritzsche, J. Electron Spectrosc. Relat. Phenom. **114-116**, 1155 (2001).
[25] S. Ricz, J. Nikkinen, R. Sankari, T. Ricsóka, Á. Kövér, D. Varga, S. Fritzsche, H. Aksela, and S. Aksela, Phys. Rev. A **72**, 014701 (2005).
[26] M. K. Inal, A. Surzhykov, and S. Fritzsche, Phys. Rev. A **72**, 042720 (2005).
[27] I. P. Grant, in *Methods in Computational Chemistry*, edited by S. Wilson (Plenum, New York, 1988), Vol. 2, p. 1.
[28] S. Fritzsche, T. Inghoff, and M. Tomaselli, Comput. Phys. Commun. **153**, 424 (2003).
[29] A. Surzhykov, P. Koval, and S. Fritzsche, Comput. Phys. Commun. **165**, 139 (2005).
[30] J. E. Sienkiewicz, S. Fritzsche, and I. P. Grant, J. Phys. B **28**, L633 (1995).
[31] A. N. Grum-Grzhimailo, S. Fritzsche, P. O'Keeffe, and M. Meyer, J. Phys. B **38**, 2545 (2005).